

---

# Tide-induced head fluctuations in a coastal aquifer: effects of the elastic storage and leakage of the submarine outlet-capping

Xiaolong Geng · Hailong Li · Michel C. Boufadel ·  
Shuang Liu

**Abstract** This paper considers the tidal head fluctuations in a single coastal confined aquifer which extends under the sea for a certain distance. Its submarine outlet is covered by a silt-layer with properties dissimilar to the aquifer. Recently, Li et al. (2007) gave an analytical solution for such a system which neglected the effect of the elastic storage (specific storage) of the outlet-capping. This article presents an analytical solution which generalizes their work by incorporating the elastic storage of the outlet-capping. It is found that if the outlet-capping is thick enough in the horizontal direction, its elastic storage has a significant enhancing effect on the tidal head fluctuation. Ignoring this elastic storage will lead to significant errors in predicting the relationship of the head fluctuation and the aquifer hydrogeological properties. Quantitative analysis shows the effect of the elastic

storage of the outlet-capping on the groundwater head fluctuation. Quantitative conditions are given under which the effect of this elastic storage on the aquifer's tide-induced head fluctuation is negligible.

**Keywords** Coastal aquifers · Elastic storage · Submarine outlet-capping · Analytical solutions · Tidal loading efficiency

## Introduction

In coastal aquifers, the groundwater head is usually influenced by many factors. Ocean tidal fluctuation is one of the most important factors and many analytical studies and field observations (e.g., Jacob (1950); Trefry and Johnston (1998); Jiao and Tang (1999); Li and Jiao (2002b); Li and Jiao (2002)) are associated with this factor. All these analytical studies have assumed a direct hydraulic connection between the aquifer's submarine outlet and the seawater.

Recently, Li et al. (2007) considered a coastal confined aquifer that extends under the sea for a certain distance with an outlet-capping. Guo et al. (2007) and Xia et al. (2007) considered multi-layered coastal leaky aquifer systems with outlet-cappings. These studies neglected the elastic storage (specific storage) of the submarine outlet-capping. Various pumping test data and field experimental studies in coastal aquifers show that if the submarine outlet-capping is comprised of thick, soft sedimentary materials, its elastic storage is much greater than that of the main aquifer (Li and Jiao (2001)). In this case, ignoring the elastic storage may lead to significant model errors.

Li and Jiao (2001) considered the elastic storage of a semi-permeable layer in a coastal aquifer system abutting a tidal water body, where the flow direction in the semi-permeable layer is vertical and there is no tidal loading effect. The study described in this article, however, relates to the effect of elastic storage of the submarine outlet-capping of a confined coastal aquifer, where the flow direction is horizontal and there is tidal loading effect. A new analytical solution has been derived. Based on this analytical solution, the influence of the elastic storage of the outlet-capping on the tidal-induced groundwater head

---

Received: 16 February 2008 / Accepted: 22 January 2009  
Published online: 17 February 2009

© Springer-Verlag 2009

---

X. Geng · H. Li · S. Liu  
Department of Mathematics,  
Anshan Normal University,  
Anshan, 114005, People's Republic of China

X. Geng  
e-mail: gengxiaolong@gmail.com

S. Liu  
e-mail: liushuang78@gmail.com

H. Li · S. Liu  
School of Environmental Studies & (MOE)  
Biogeology and Environmental Geology Lab,  
China University of Geosciences,  
Wuhan, 430074, People's Republic of China

H. Li (✉) · M. C. Boufadel  
Department of Civil and Environmental Engineering,  
Temple University,  
1947 N 12th Street, Philadelphia, PA 19122, USA  
e-mail: hailong@temple.edu  
Tel.: +01-215-2048428  
Fax: +01-215-2044696

M. C. Boufadel  
e-mail: boufadel@temple.edu

fluctuation is discussed. Quantitative conditions are also discussed under which the effect of this elastic storage on the aquifer's tide-induced head fluctuation is negligible.

**Mathematical model and analytical solution**

A coastal confined aquifer is considered, which has an impermeable roof that extends under the sea for a distance  $L$ . The aquifer's submarine outlet is covered by a different layer of sediment (Fig. 1). Following Li et al. (2007), the following assumptions will be used: The confined aquifer is horizontal and extends landward infinitely. The roof and bottom of the confined aquifer are impermeable. Both the confined aquifer and its outlet-capping are homogeneous, isotropic and have constant thickness. The flow is horizontal in the coastal aquifer system and follows Darcy's law. The density difference between the groundwater and the seawater is neglected owing to its slight impact on groundwater level fluctuation.

Let the  $x$ -axis be positive landward and perpendicular to the coastline, and the intersection with the coastline be the origin of the axis (Fig. 1). According to the above assumptions, the groundwater flow is governed by the following equations.

1. Groundwater flow in the inland aquifer:

$$S_s \frac{\partial h}{\partial t} = K \frac{\partial^2 h}{\partial x^2}, x > 0, \tag{1}$$

2. Groundwater flow in the offshore aquifer:

$$S_s \frac{\partial h}{\partial t} = K \frac{\partial^2 h}{\partial x^2} + S_s L_e \frac{\partial h_s}{\partial t}, -L < x < 0, \tag{2}$$

where  $h(x, t)$ ,  $K$  and  $S_s$  are the hydraulic head [L], hydraulic conductivity [ $L T^{-1}$ ] and specific storage [ $L^{-1}$ ]

of the confined aquifer, respectively;  $h_s$  is the head of seawater [L] and defined as

$$h_s(t) = A \cos(\omega t), \tag{3}$$

where  $A$  is the tidal amplitude [L],  $\omega = 2\pi/t_0$  is the tidal frequency [ $T^{-1}$ ],  $t_0$  is the tidal period [T].  $L_e$  is the loading efficiency (dimensionless) of the sea tide (Jacob 1950) on the confined aquifer and defined as

$$L_e = \alpha / (\alpha + n\beta), \tag{4}$$

where  $\alpha$  is the compressibility [ $M^{-1}LT^2$ ] of the confined aquifer's skeleton,  $\beta$  is the compressibility [ $M^{-1}LT^2$ ] of the pore water in the confined aquifer, and  $n$  is the porosity (dimensionless) of the aquifer.

3. Groundwater flow in the submarine outlet-capping:

$$S_{s1} \frac{\partial h_1}{\partial t} = K_1 \frac{\partial^2 h_1}{\partial x^2} + S_{s1} L_{e1} \frac{\partial h_s}{\partial t}, -(L + m) < x < -L, \tag{5}$$

where  $h_1(x, t)$ ,  $K_1$  and  $S_{s1}$  are the hydraulic head [ $L^{-1}$ ], hydraulic conductivity [ $L T^{-1}$ ] and specific storage [ $L^{-1}$ ] of the outlet-capping, respectively;  $m$  is the horizontal thickness of the outlet-capping;  $L_{e1}$  is the loading efficiency (dimensionless) of the sea tide on the outlet-capping and defined as

$$L_{e1} = \alpha_1 / (\alpha_1 + n_1\beta), \tag{6}$$

where  $\alpha_1$  is the compressibility [ $M^{-1}LT^2$ ] of the skeletal outlet-capping, and  $n_1$  is the porosity (dimensionless) of the outlet-capping.

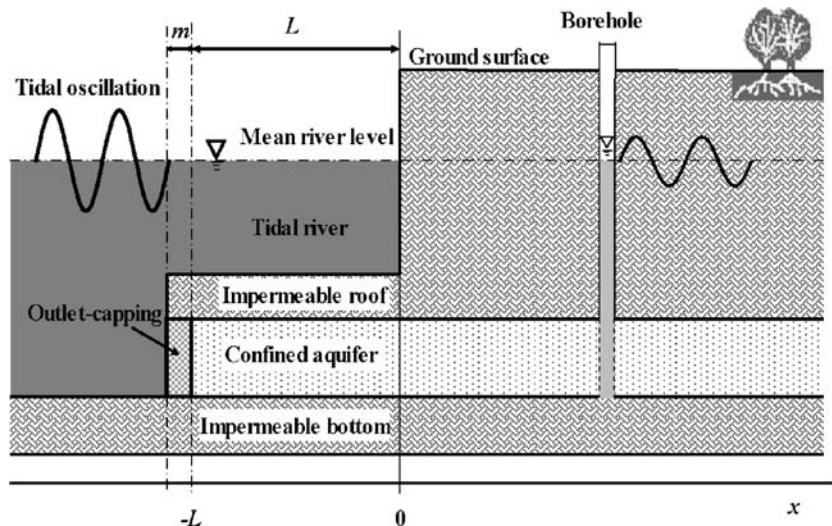


**Fig. 1** Schematic of the cross-section of a coastal confined aquifer which extends under the sea for a certain distance with a silt-layer outlet-capping

At inland places far from the coastline, no-flow boundary condition is used

$$\lim_{x \rightarrow \infty} \frac{\partial h}{\partial x} = 0. \tag{7}$$

At the coastline  $x=0$  and the interface of the offshore aquifer and the outlet-capping  $x=-L$ , using the continuities of hydraulic head and flux, respectively, one has

$$\lim_{x \rightarrow 0^-} h(x, t) = \lim_{x \rightarrow 0^+} h(x, t), \tag{8}$$

$$\lim_{x \rightarrow 0^-} \frac{\partial h}{\partial x} = \lim_{x \rightarrow 0^+} \frac{\partial h}{\partial x}, \tag{9}$$

$$\lim_{x \rightarrow -L^-} h_1(x, t) = \lim_{x \rightarrow -L^+} h(x, t), \tag{10}$$

$$\lim_{x \rightarrow -L^-} K_1 \frac{\partial h_1}{\partial x} = \lim_{x \rightarrow -L^+} K \frac{\partial h}{\partial x}. \tag{11}$$

At the interface of the seawater and the outlet-capping, a Dirichlet boundary condition is used

$$h_1(x, t)|_{x=-(m+L)} = h_S(x, t). \tag{12}$$

For sake of convenience, three parameters are introduced here:

$$a = \sqrt{\frac{\omega S_s}{2K}} = \sqrt{\frac{\pi S_s}{K t_0}}, \tag{13}$$

$$\theta = m \sqrt{\frac{\omega S_{s1}}{2K_1}} = m \sqrt{\frac{\pi S_{s1}}{K_1 t_0}} \tag{14}$$

$$\sigma = \frac{K_1}{amK} = \frac{K_1}{m} \sqrt{\frac{t_0}{\pi S_s K}} \tag{15}$$

Here  $a$  is the tidal propagation parameter of the confined aquifer [ $L^{-1}$ ],  $\theta$  and  $\sigma$  are the dimensionless buffer capacity and the dimensionless relative leakance of the submarine outlet-capping, respectively.

The derivations of  $h(x,t)$  and  $h_1(x,t)$  are detailed in Appendix A. The hydraulic head  $h(x,t)$  in the confined aquifer reads:

$$h(x, t) = AL_e \left[ \cos(\omega t) - \frac{1}{2} e^{ax} \cos(\omega t + ax) + h_0(x, t) \right], \tag{16}$$

$$-L < x < 0,$$

$$h(x, t) = AL_e \left[ \frac{1}{2} e^{ax} \cos(\omega t - ax) + h_0(x, t) \right], \quad x > 0. \tag{17}$$

where

$$h_0(x, t) = |C_2| e^{-ax} \cos(\omega t - ax + \arg C_2), \tag{18}$$

where

$$C_2 = C_2(L_e, L_{e1}, \theta, \sigma, aL) = \frac{L_e}{2} \frac{\theta \sigma \operatorname{ch}(\Delta) - \operatorname{sh}(\Delta)}{\theta \sigma \operatorname{ch}(\Delta) + \operatorname{sh}(\Delta)} e^{-2aL(1+i)} + \frac{\theta \sigma [(L_{e1} - L_e) \operatorname{ch}(\Delta) + (1 - L_{e1})]}{\theta \sigma \operatorname{ch}(\Delta) + \operatorname{sh}(\Delta)} e^{-aL(1+i)}, \tag{19}$$

with

$$\Delta = \theta(1 + i). \tag{20}$$

### Discussion

Recently, Li et al. (2007) gave an analytical solution for a special case of models of Eqs. (1)–(11) when  $S_{s1} = 0$  (i.e., the effect of the elastic storage of the outlet-capping is neglected). When  $S_{s1} = 0$  or equivalently  $\theta = 0$ , Eq. (16) described here collapses into that by Li et al. (2007; Eq. (9) of their paper). So the model error caused by ignoring the effect of the outlet-capping’s elastic storage is given by the difference between Eq. (16) described here and that of Li et al. (2007). Because both solutions have the same governing equations—Eqs. (1) and (2)—for the aquifer’s domain  $-L < x < \infty$  and the same boundary condition at  $x = \infty$ , Eq. (7), and interface conditions at  $x = 0$ —Eqs. (8) and (9)—using the “extremum principle” (see Ockendon et al. 1999), the maximum of the difference of the two solutions will be reached at the left end  $x = -L$  of the domain  $-L < x < \infty$ , namely, at the interface of the aquifer

and the outlet-capping. Therefore, the maximum model error reaches  $x=-L$  at the interface and can be written as (see Appendix B for details derivation):

$$E_{\max}(\theta, \sigma, aL, L_e, L_{e1}) = e^{aL} \left| \left( \lim_{\theta \rightarrow 0^+} C_2 \right) - C_2 \right|; \quad (21)$$

here the periodicity of the solutions is used.

Compared with the solution of Li et al. (2007), the new Eq. (16) considers the buffer capacity  $\theta$  and the loading efficiency  $L_{e1}$  of the outlet-capping. In the discussions below, it is assumed that the properties of the submarine outlet-capping are similar to the semi-permeable layers in the case study examples summarized by Li and Jiao (2001). Using the data of the specific storage and hydraulic conductivity in Table 1 of Li and Jiao (2001), the value of  $\theta$  for a unit thickness ( $m=1$  m) ranges from 0.2 to 2.5 for diurnal or semidiurnal tidal frequencies. Thus,  $\theta$  will range from 0.0 to 25 when the thickness  $m$  ranges from 0.1 to 10 m. As will be shown later, the buffer capacity has a threshold value of 0.5 in the sense that, if  $\theta \leq 0.5$ , the elastic storage effect can be neglected. Therefore, the discussion here will only focus on a narrow but more important value range of  $\theta \in [0, 2]$  near the threshold value. Because the compressibility ( $\alpha_1$ ) of the soft submarine sedimentary materials of the submarine outlet-capping (such as silt and fine sand) is several orders of magnitudes greater than the compressibility of water ( $\beta$ ) (Freeze and Cherry (1979), Table 2.5), and  $n_1 < 1$ , Eq. (6) usually gives a value of  $L_{e1}$  very close to 1. Due to this, the value of  $L_{e1}$  will be fixed at 1.0 in the following discussion. Field observations—e.g., Gregg (1966), Fig. 6; Carr and van der Kamp (1969), Table 2; Erskine (1991), Figs. 4–6—and theoretical analysis of Merritt

(2004) demonstrate that the typical value of  $L_e$  ranges from 0.05 to 1. In the discussion, three values 0.1, 0.5 and 0.9 will be used for  $L_e$ . For the dimensionless extending length  $aL$ , three different values 0.0, 1.0 and 4.0 will be used in the discussion, representing, respectively, zero, intermediate and long offshore extending lengths.

Figure 2 shows how the ratio  $E_{\max}/A$  of the maximum error to the tidal amplitude changes with  $\sigma$  for different values of  $\theta$  when  $L_{e1}=1.0, aL=0$ . For any fixed value of  $\theta$ . The error  $E_{\max}$  increases with the dimensionless buffer capacity  $\theta$ , and is a mono-peak function of the dimensionless relative leakance  $\sigma$  with the maximums occurring near  $\sigma=1$  and tending to zero rapidly when  $\sigma$  is much less than or much greater than 1.0. The errors are less than 5% when either  $\sigma \leq 0.03$ , or  $\sigma \geq 11$ , or  $\sigma \leq 0.5$ .

Figure 3 shows how the ratio  $E_{\max}/A$  of the maximum error to the tidal amplitude changes with  $\sigma$  for different values of  $\theta$  and  $L_e$  ( $\theta=0.5, 1.0, 2.0; L_e=0.1, 0.5, 0.9$ ) when  $L_{e1}=1.0, aL=1.0$ . For any fixed value of  $\theta$ ,  $E_{\max}$  increases with the dimensionless buffer capacity  $\theta$ , decreases with the loading efficiency  $L_e$  of the offshore aquifer and is a mono-peak function of the dimensionless relative leakance  $\sigma$  with the maximums occurring near  $\sigma=1$  and tending to zero rapidly when  $\sigma$  is much less than or much greater than 1.0. The errors are less than 5% when either  $\sigma \leq 0.03$ , or  $\sigma \geq 11$ , or  $\theta \leq 0.5$  or any value of  $L_e$ . Compared with Fig. 2, the effect of the offshore aquifer extending length  $aL$  on the maximum error  $E_{\max}$  is weak. Figure 4 is the case when  $aL=4.0$ . Compared with Fig. 3, the maximum error  $E_{\max}$  is almost insensitive to the change of  $aL$ .

From this discussion, one can conclude that the effect of the elastic storage of the outlet-capping on the head fluctuation can be ignored when the dimensionless buffer capacity  $\theta$  is small ( $\theta \leq 0.5$ ) and/or  $\sigma$  is much less than or much greater than 1.0.

Two hypothetical examples are designed to clearly demonstrate the effect of elastic storage of outlet-capping

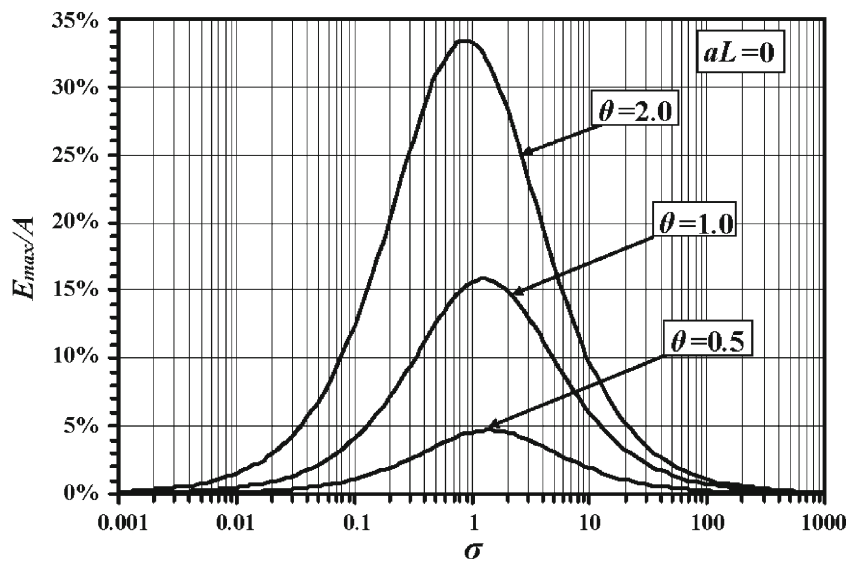


Fig. 2 Changes of the maximum relative error  $E_{\max}(\theta, \sigma, aL, L_e, L_{e1})$  with  $\sigma$  for different values of  $\theta$  when  $L_{e1}=1.0, aL=0$

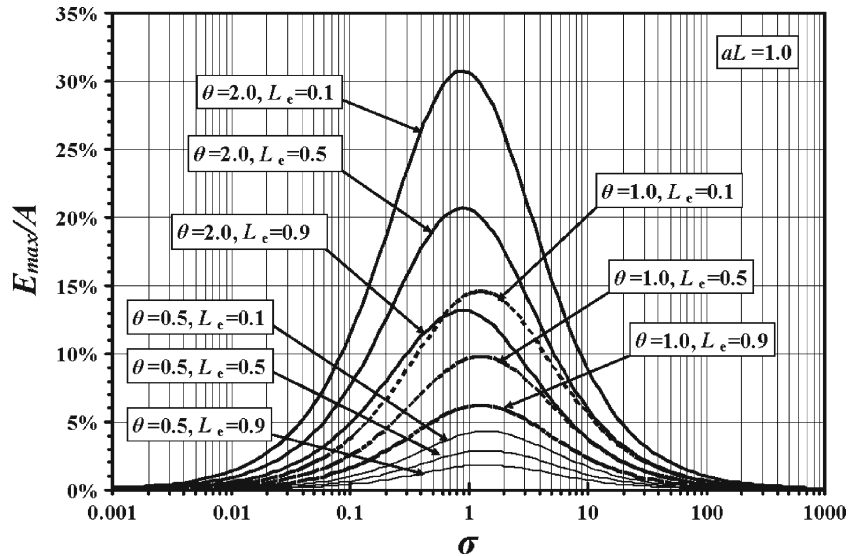


Fig. 3 Changes of the maximum relative error  $E_{\max}(\theta, \sigma, aL, L_e, L_{e1})$  with  $\sigma$  for different values of  $\theta$  and  $L_e$  when  $L_{e1}=1.0$  and  $aL=1.0$

on the tide-induced groundwater head under the different conditions. The thicknesses, hydraulic conductivities and specific storages of the aquifer and the outlet-capping are listed in Table 1. These values are within the value ranges of the real coastal aquifer systems reported in literature, which were summarized in Table 1 of Li and Jiao (2001). The properties of the outlet-capping are assumed to be similar to those of the aquitards listed in Table 1 of Li and Jiao (2001) and the offshore extending length  $L$  is zero. The tidal period is 12.4 h (semidiurnal). Figure 5 shows the tidal level and head fluctuations predicted by Eq. (16) and the solution of Li et al. (2007) at the coastline  $x=0$  of the aquifer of “example 1” in Table 1. One can see that the effect of the elastic storage of the outlet-capping for example 1 is significant and neglecting the elastic storage

will lead to model error of 27.1%. An apparently strange phenomenon shown in Fig. 5 is that the tide-induced head fluctuation amplitude is underestimated by the solution of Li et al. (2007), which ignores the elastic storage of the outlet-capping. Physically, due to the elastic storage of the outlet-capping, the pore water out of the elastic storage of the outlet-capping can be squeezed into the aquifer during the rising tide and conversely during falling tide. As a result, the neglect of the elastic storage of the outlet-capping will underestimate the water volume through the interface of the outlet-capping or equivalently underestimate the head fluctuation at the interface. In other words, the elastic storage of the outlet-capping has an enhancing effect on the tidal head fluctuation. This effect is neglected in the Li et al. (2007) solution because they ignored the

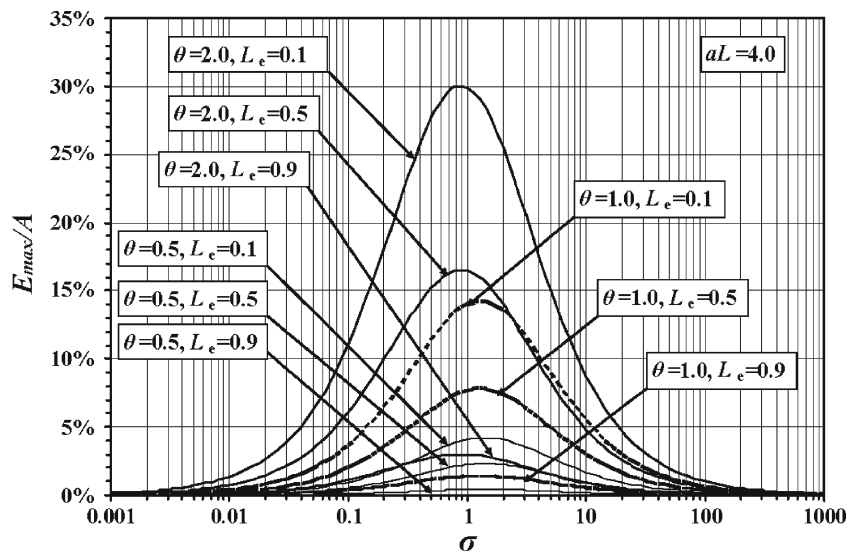


Fig. 4 Changes of the maximum relative error  $E_{\max}(\theta, \sigma, aL, L_e, L_{e1})$  with  $\sigma$  for different values of  $\theta$  and  $L_e$  when  $L_{e1}=1.0$  and  $aL=4.0$

**Table 1** Parameters and maximum model errors of two hypothetical examples of confined aquifer systems

Example	Confined aquifers			Outlet-capping			$\theta$	$\sigma$	$E_{\max}/A$
	$K$ (m day <sup>-1</sup> )	$S_s$ (L <sup>-1</sup> )	$b^a$ (m)	$K_1$ (m day <sup>-1</sup> )	$S_{s1}$ (L <sup>-1</sup> )	$m$ (m)			
1	11.4	0.000002	10	0.009	0.0015	9	1.85	0.416	27.1%
2	7.714	0.00000257	14	0.013	0.00025	4	0.279	1.45	1.5%

<sup>a</sup>Here  $b$  is the vertical thickness of the confined aquifer

elastic storage of the outlet-capping. Another noticeable phenomenon is that the head predicted by Eq. (16) at  $x=0$  fluctuates with a negative phase shift, i.e., the peak of the head fluctuation is a little bit in advance of that of the tidal fluctuation. This is caused by the combined effects of elastic storage of the outlet-capping and the tidal loading over the outlet-capping. Figure 6 shows the results for example 2 where the effect of the elastic storage of the outlet-capping is negligible (the model error is 1.5%). One can see the two curves predicted by Eq. (16) and the solution of Li et al. (2007) almost coincide with each other.

## Conclusions

The submarine outlet of a coastal confined aquifer is usually covered by a layer of sediment different from the aquifer (outlet-capping). Previous researchers neglected the effect of the elastic storage of the outlet-capping. This article discusses an analytical study of the effect of the elastic storage of the outlet-capping. It is found that the elastic storage of the outlet-capping has an enhancing effect on the tidal head fluctuation. The model error caused by neglecting the effect of the elastic storage of the outlet-capping was analyzed: it increases with the dimensionless buffer capacity  $\theta$ , and is a mono-peak function of the dimensionless relative leakage  $\sigma$  with the maximums occurring near  $\sigma=1$  and tending to zero rapidly when  $\sigma$  is much less than or much greater than 1.0. The error is less

than 5% when either  $\sigma \leq 0.03$ , or  $\sigma \leq 11$ , or  $\sigma \leq 0.5$ ; in other words, it is negligible if the outlet-capping is either (1) sufficiently thin in horizontal direction and/or close to the aquifer in permeability; or (2) sufficiently thick in horizontal direction and/or much less permeable than the aquifer; or (3) the elastic storage of the outlet-capping is small.

**Acknowledgements** This research is supported by National Natural Science Foundation of China (No. 40672167) and the 111 Project (B08030). We are grateful to the Managing Editor and two anonymous reviewers for their helpful comments.

## Appendix A: Derivation of the solution

Suppose

$$h(x, t) = \text{Re}[H(x, t)] = A \text{Re}[X(x)e^{i\omega t}], \quad (22)$$

$$h_1(x, t) = \text{Re}[H_1(x, t)] = A \text{Re}[X_1(x)e^{i\omega t}], \quad (23)$$

where  $X(x)$ ,  $X_1(x)$  are complex functions.  $\text{Re}$  denotes the real part of the followed complex expression,  $i = \sqrt{-1}$ . Substituting Eqs. (22) and (23) back into

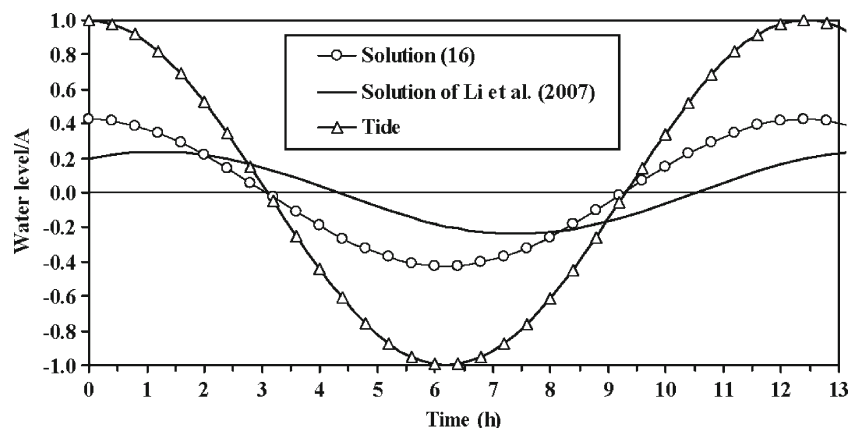


**Fig. 5** The tide-induced head fluctuations with time predicted by Eq. (16) and the solution of Li et al. (2007) at the coastline  $x=0$  of example 1 in Table 1. The semidiurnal tide is also shown for comparison

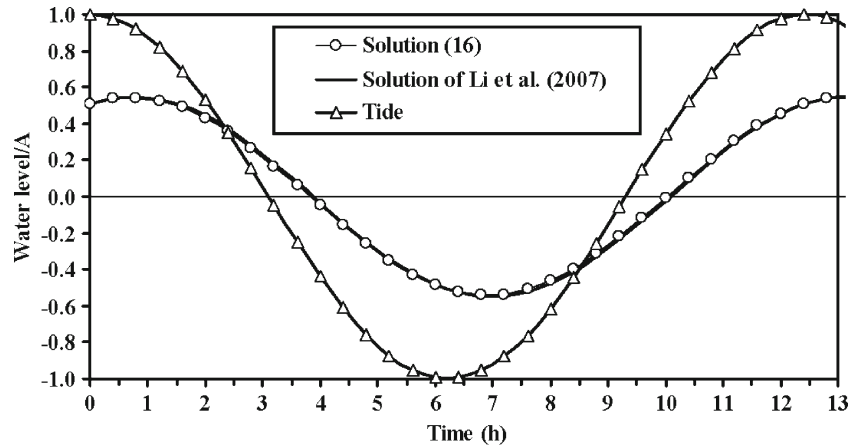


**Fig. 6** The tide-induced head fluctuations with time predicted by Eq. (16) and the solution of Li et al. (2007) at the coastline  $x=0$  of example 2 in Table 1. The semidiurnal tide is also shown for comparison

Eqs. (1), (2), (5), (7)–(12) and then extending the equations into complex ones with respect to  $X(x)$ , yields

$$i\omega S_s X(x) = KX''(x), \quad x > 0, \tag{24}$$

$$i\omega S_s X(x) = KX''(x) + i\omega L_e S_s, \quad -L, < x < 0, \tag{25}$$

$$i\omega S_{s1} X_1(x) = KX_1''(x) + i\omega L_{e1} S_{s1}, \tag{26}$$

$$-(L + m) \leq x < -L,$$

$$\lim_{x \rightarrow \infty} X'(x) = 0, \tag{27}$$

$$X_1(x)|_{x=-(m+L)} = 1, \tag{28}$$

$$\lim_{x \rightarrow 0^-} X(x) = \lim_{x \rightarrow 0^+} X(x), \tag{29}$$

$$\lim_{x \rightarrow 0^-} X'(x) = \lim_{x \rightarrow 0^+} X'(x), \tag{30}$$

$$\lim_{x \rightarrow -L^-} X_1(x) = \lim_{x \rightarrow -L^+} X(x), \tag{31}$$

$$\lim_{x \rightarrow -L^-} K_1 X_1'(x) = \lim_{x \rightarrow -L^+} KX'(x). \tag{32}$$

The general solutions to Eqs. (33)–S(35) are

$$X(x) = C_1 e^{a(1+i)x} + C_2 e^{-a(1+i)x} + L_e, \tag{33}$$

$$-L < x < 0,$$

$$X(x) = C_3 e^{a(1+i)x} + C_4 e^{-a(1+i)x}, \quad x > 0, \tag{34}$$

$$X_1(x) = C_5 e^{\frac{a}{m}(1+i)x} + C_6 e^{-\frac{a}{m}(1+i)x} + L_e, \tag{35}$$

$$-(L + m) \leq x < -L,$$

where  $C_1, C_2, C_3, C_4, C_5$  and  $C_6$  are six unknown complex constants. By means of Eqs. (27)–(32), after some routine calculation, one obtains

$$C_1 = -\frac{L_e}{2}, \tag{36}$$

$$C_3 = 0, \tag{37}$$

$$C_4 = C_2 + \frac{1}{2}L_e, \tag{38}$$

$$C_5 = \frac{1}{2\theta\sigma} e^{\frac{L_e \Delta}{m}} \left[ (\theta\sigma - 1)C_2 e^{aL(1+i)} - \frac{1}{2}(\theta\sigma + 1)L_e e^{-aL(1+i)} + \theta\sigma(L_e - L_{e1}) \right], \tag{39}$$

$$C_6 = \left[ (1 - L_{e1}) - C_5 e^{-(1+\frac{L}{m})\Delta} \right] e^{-(1+\frac{L}{m})\Delta}, \quad (40)$$

and  $C_2$  is given by Eq. (19)

Substituting Eqs. (36)–(37), Eq. (19) into Eqs. (24)–(35), one can obtain  $X(x)$ ,  $X_1(x)$ . Substituting the resultant expression of  $X_1(x)$  into  $H_1(x,t)$ , and calculating the real part of  $H_1(x,t)$ , one finally obtains the solution:

$$h_1(x,t) = e^{\frac{\theta}{m}(x+L)} |C_5| \cos\left(\omega t + \frac{\theta}{m}(x+L) - \arg C_5\right) - (L+m) < x < -L. \quad (41)$$

$$+ e^{\left(-\frac{\theta}{m}(x+L)\right)} |C_6| \cos\left(\omega t - \frac{\theta}{m}(x+m+L) - \arg C_6\right) + L_{e1} \cos(\omega t),$$

Substituting the resultant expression of  $X(x)$  into  $H(x,t)$ , and calculating the real part of  $H(x,t)$ , one finally obtains the Eqs. (16) and (17).

## Appendix B: Derivation of the maximum relative error

Using Eqs. (16) and (18), the difference  $E$  of the Eq. (16) and that of Li et al. (2007) at the interface  $x=-L$  can be expressed as

$$E/A = \lim_{\theta \rightarrow 0^+} [|C_2| e^{aL} \cos(\omega t - ax + \arg C_2)] - |C_2| e^{aL} \cos(\omega t - ax + \arg C_2)$$

$$= e^{aL} \operatorname{Re} \left\{ \lim_{\theta \rightarrow 0^+} C_2 e^{i(\omega t - ax)} - C_2 e^{i(\omega t - ax)} \right\} \leq e^{aL} \left| \lim_{\theta \rightarrow 0^+} C_2 e^{i(\omega t - ax)} - C_2 e^{i(\omega t - ax)} \right| \quad (42)$$

$$= e^{aL} \left| \lim_{\theta \rightarrow 0^+} C_2 - C_2 \right|.$$

One is always able to chose the value of  $t$  so that the imaginary part of  $\lim_{\theta \rightarrow 0^+} C_2 e^{i(\omega t - ax)} - C_2 e^{i(\omega t - ax)}$  vanishes and the inequality (Eq. 42) becomes an equality. So the maximum error  $E_{max}(\theta, \sigma, aL, L_e, L_{e1})$  is given by Eq. (21).

## References

- Carr PA, van der Kamp GS (1969) Determining aquifer characteristics by the tidal methods. *Water Resour Res* 5(5):1023–1031
- Erskine AD (1991) The effect of tidal fluctuation on a coastal aquifer in the UK. *Ground Water* 29(4):556–562
- Freeze RA, Cherry JA (1979) *Groundwater*. Prentice-Hall, Englewood Cliffs, NJ
- Gregg DO (1966) An analysis of ground-water fluctuations caused by ocean tides in Glynn County, Georgia. *Ground Water* 4(3):24–32
- Guo QN, Li HL, Xia YQ, Li GH (2007) Tide-induced groundwater head fluctuation in coastal multi-layered aquifer systems with a submarine outlet-capping. *Adv Water Resour* 30:1746–1755
- Jacob CE (1950) Flow of groundwater. In: Rouse H (ed) *Engineering hydraulics*. Wiley, New York 321–386 pp
- Jiao JJ, Tang ZH (1999) An analytical solution of groundwater response to tidal fluctuation in a leaky confined aquifer. *Water Resour Res* 35(3):747–751
- Li HL, Jiao JJ (2001) Analytical studies of groundwater-head fluctuation in a coastal confined aquifer overlain by a semi-permeable layer with storage. *Adv Water Resour* 24(5):565–573
- Li HL, Jiao JJ (2002) Analytical solutions of tidal groundwater flow in coastal two-aquifer system. *Adv Water Resour* 25(4):417–426
- Li HL, Jiao JJ, Luk M, Cheung K (2002) Tide-induced groundwater level fluctuation in coastal aquifers bounded by an L-shaped coastline. *Water Resour Res* 38(3), 1024. doi:10.1029/2001WR000556
- Li HL, Li GY, Chen JM, Boufadel MC (2007) Tide-induced head fluctuations in a confined aquifer with sediment covering its outlet at the sea floor. *Water Resour Res*. 43(3), W03404. doi:10.1029/2005WR004724
- Merritt ML (2004) Estimating hydraulic properties of the floridan aquifer system by analysis of earth-tide, ocean-tide, and barometric effects, Collier and Henry counties, Florida. *US Geol Surv Water Resour Invest Rep* 4203-4267
- Ockendon J, Howison S, Lacey A, Movchan A (1999) *Applied partial differential equations*. Oxford University Press, New York
- Trefry MG, Johnston CD (1998) Pumping test analysis for a tidally forced aquifer. *Ground Water* 36:427–33
- Xia YQ, Li HL, Boufadel MC, Guo QN, Li GH (2007) Tidal wave propagation in a coastal aquifer: effects of leakage through its submarine outlet and offshore roof. *J Hydrol* 337:249–257